1 Introduction

We include in this supporting material additional figures illustrating the influence of the new parameterization of LNO_x production (Bucsela et al., 2019, Fig. 11(c)). in the chemistry of the atmosphere. Figure S1 shows the annual spatial distribution of LNO_x. Figures S2-S10 show the annually and globally averaged differences of the NO_x, O_3, CO, HO_x, HNO_3 and HNO_4 mixing ratios between the control simulations and the simulations using the new parameterization of LNO_x production at different pressure levels and by using different lightning parameterizations. Figures S11-S12 show the impact of LNO_x on the HO_x mixing ratio in the geographical region of Europe (bounded by 42°N and 52°N latitude degrees, and 0° to 24°E longitude degrees) at the 200 hPa and the 600 hPa pressure levels, respectively. Finally, Figures S13-S24 show the monthly averaged total O_3 column in 2004 from the control simulations.

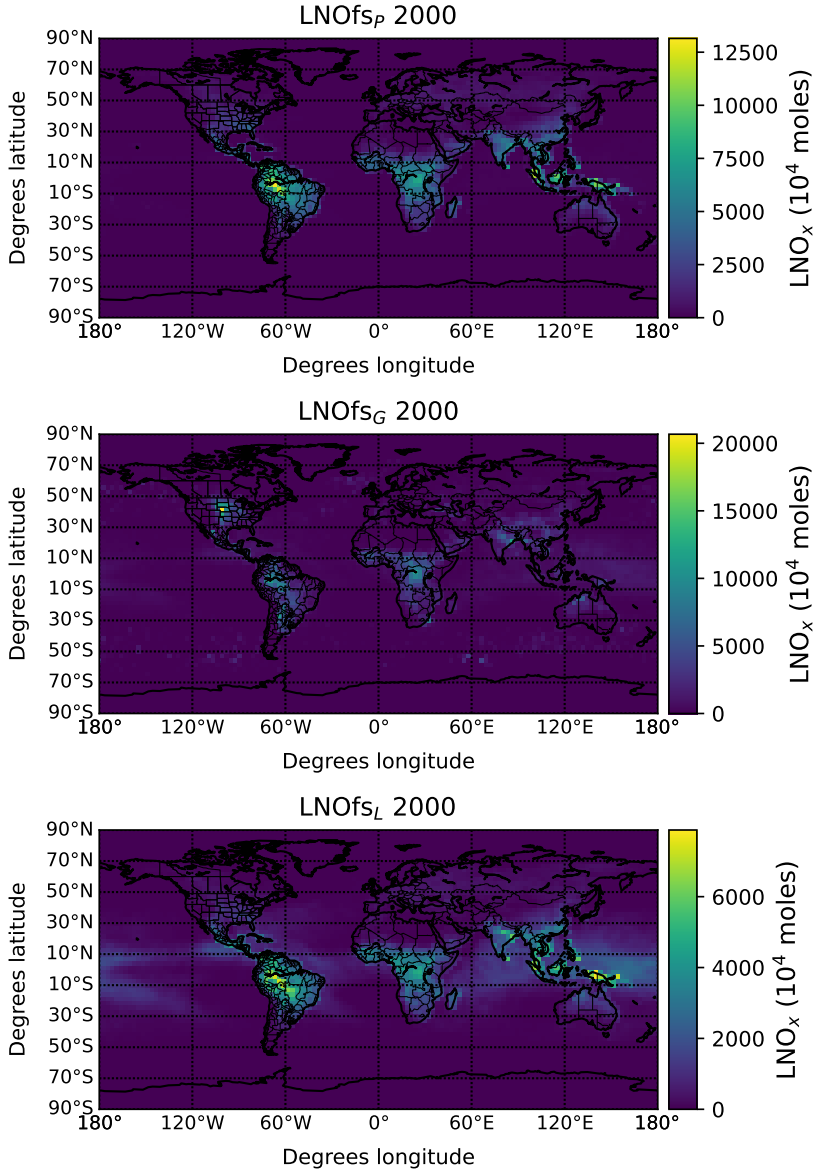

Figure S1. Comparison of spatial distribution of the mean monthly LNO_x during 2000 between the LNOfs simulations.

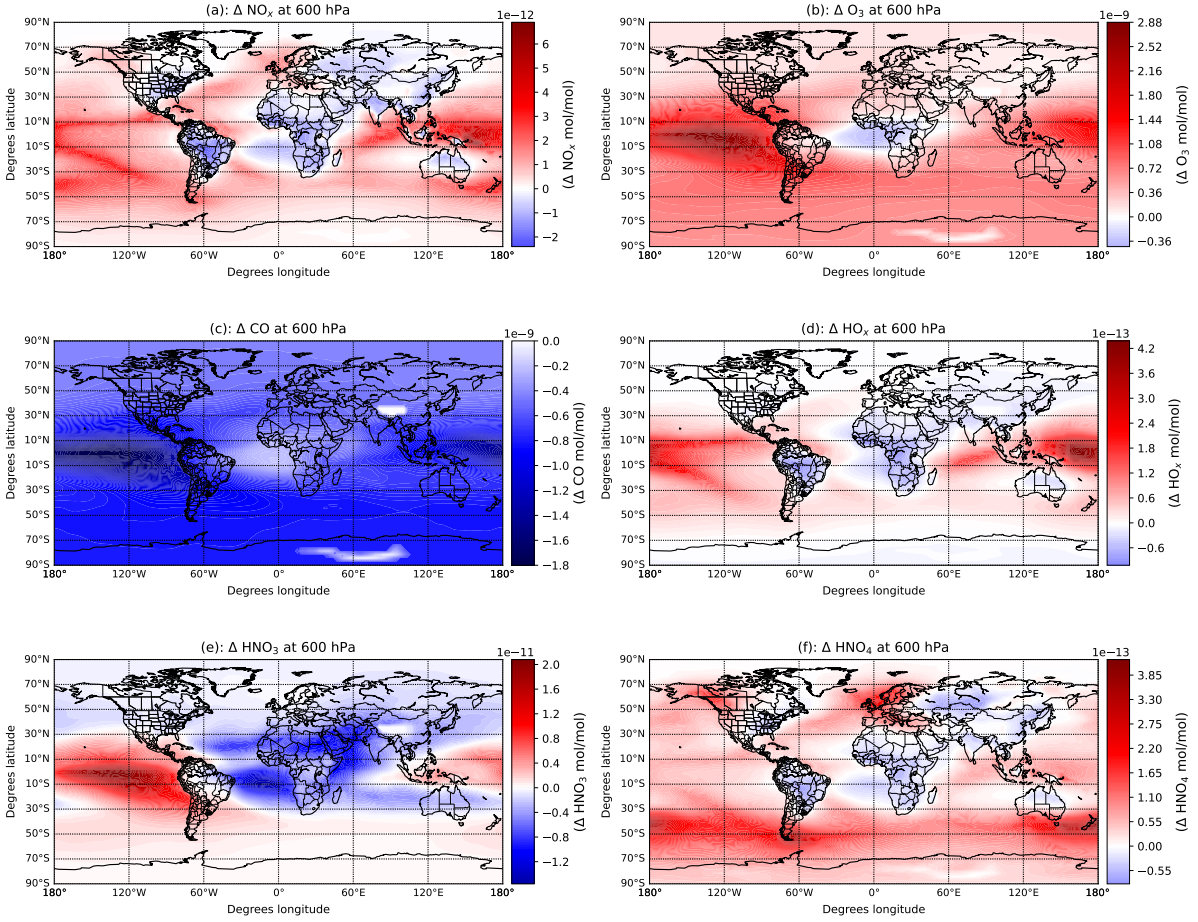

Figure S2. Annually (2002-2007) and globally averaged differences of the NO_x, O_3, CO, HO_x, HNO_3 and HNO_4 mixing ratios between the simulation with the LNO_x based on the flash frequency ($LNOfs_P$) and the simulation with a constant quantity of the LNO_x per flash (CTR_P) at 600 hPa vertical levels.

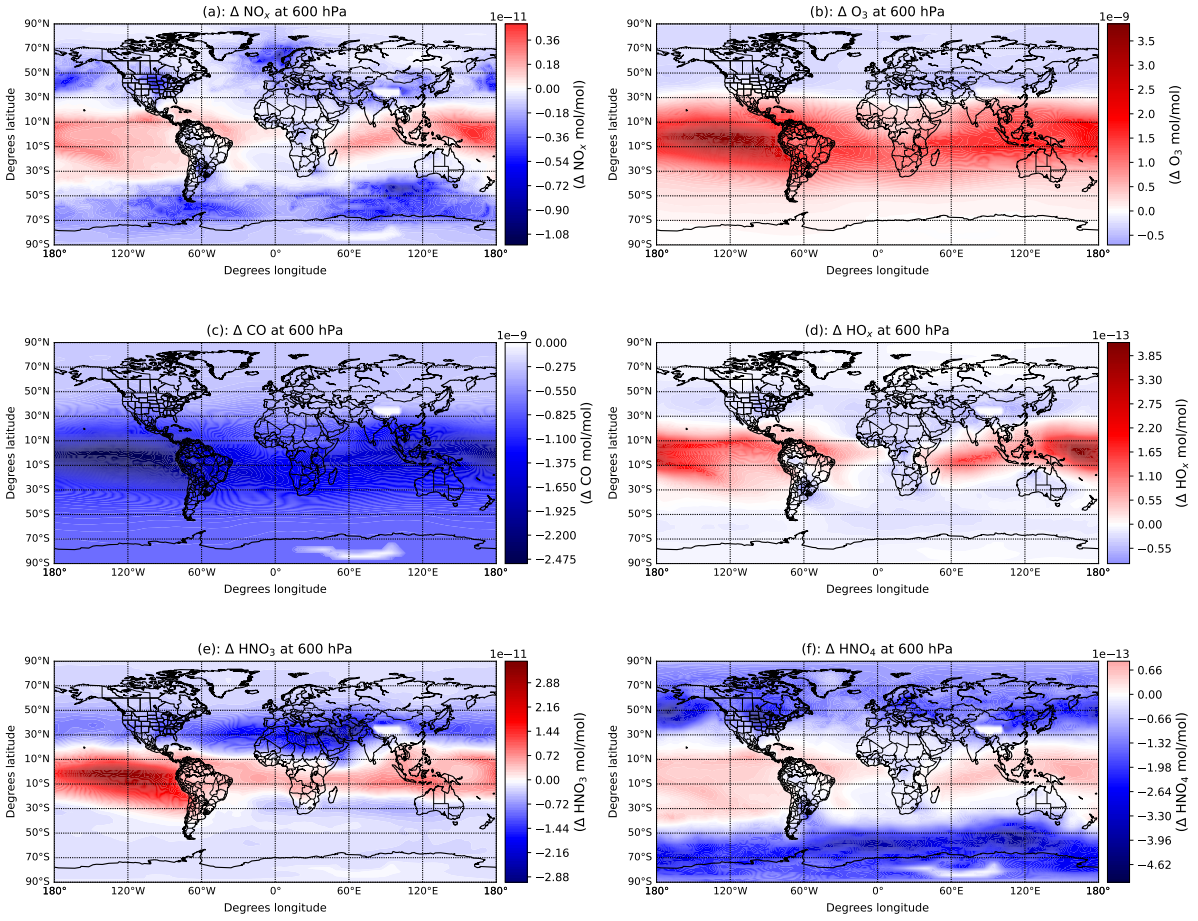

Figure S3. Annually (2002-2007) and globally averaged differences of the NO_x, O_3, CO, HO_x, HNO_3 and HNO_4 mixing ratios between the simulation with the LNO_x based on the flash frequency ($LNOfs_G$) and the simulation with a constant quantity of the LNO_x per flash (CTR_G) at 600 hPa vertical levels.

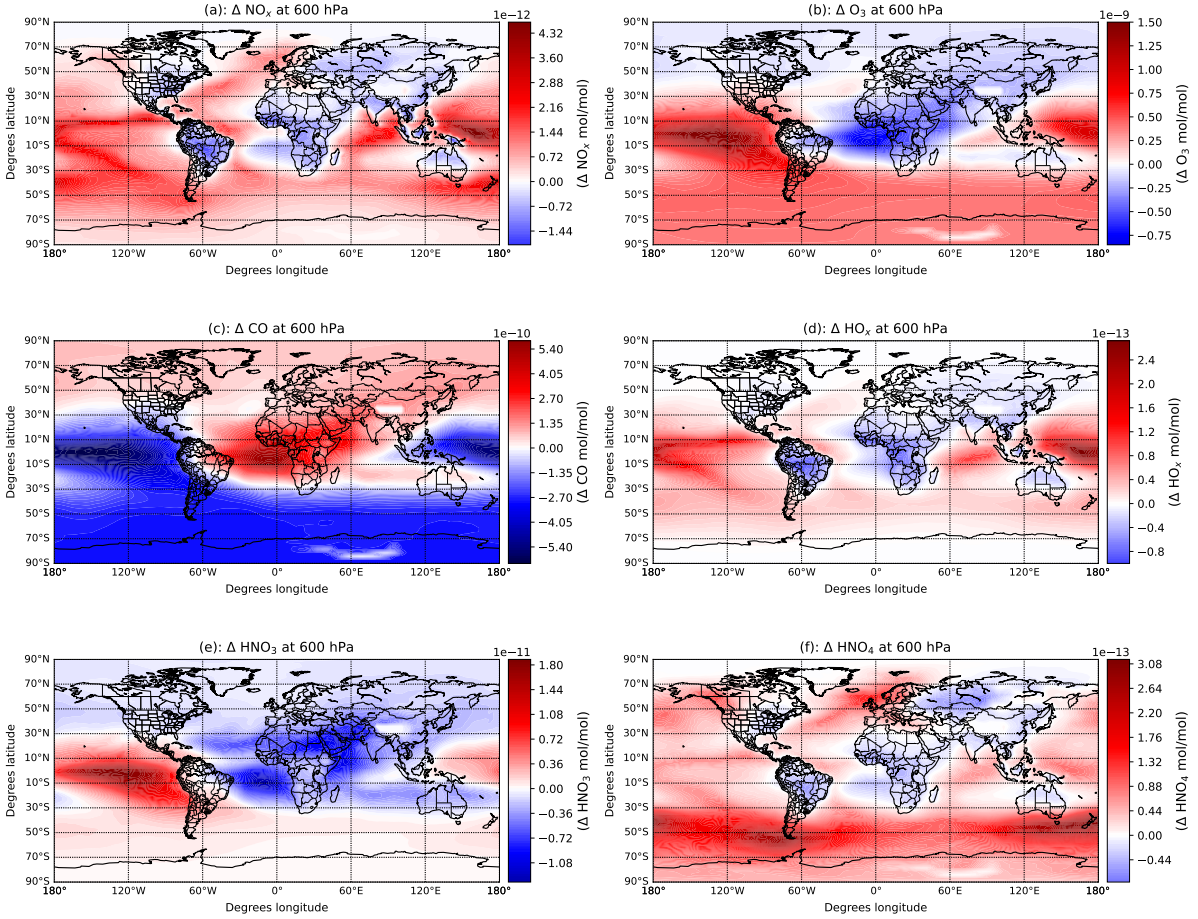

Figure S4. Annually (2002-2007) and globally averaged differences of the NO_x, O_3, CO, HO_x, HNO_3 and HNO_4 mixing ratios between the simulation with the LNO_x based on the flash frequency ($LNOfs_L$) and the simulation with a constant quantity of the LNO_x per flash (CTR_L) at 600 hPa vertical levels.

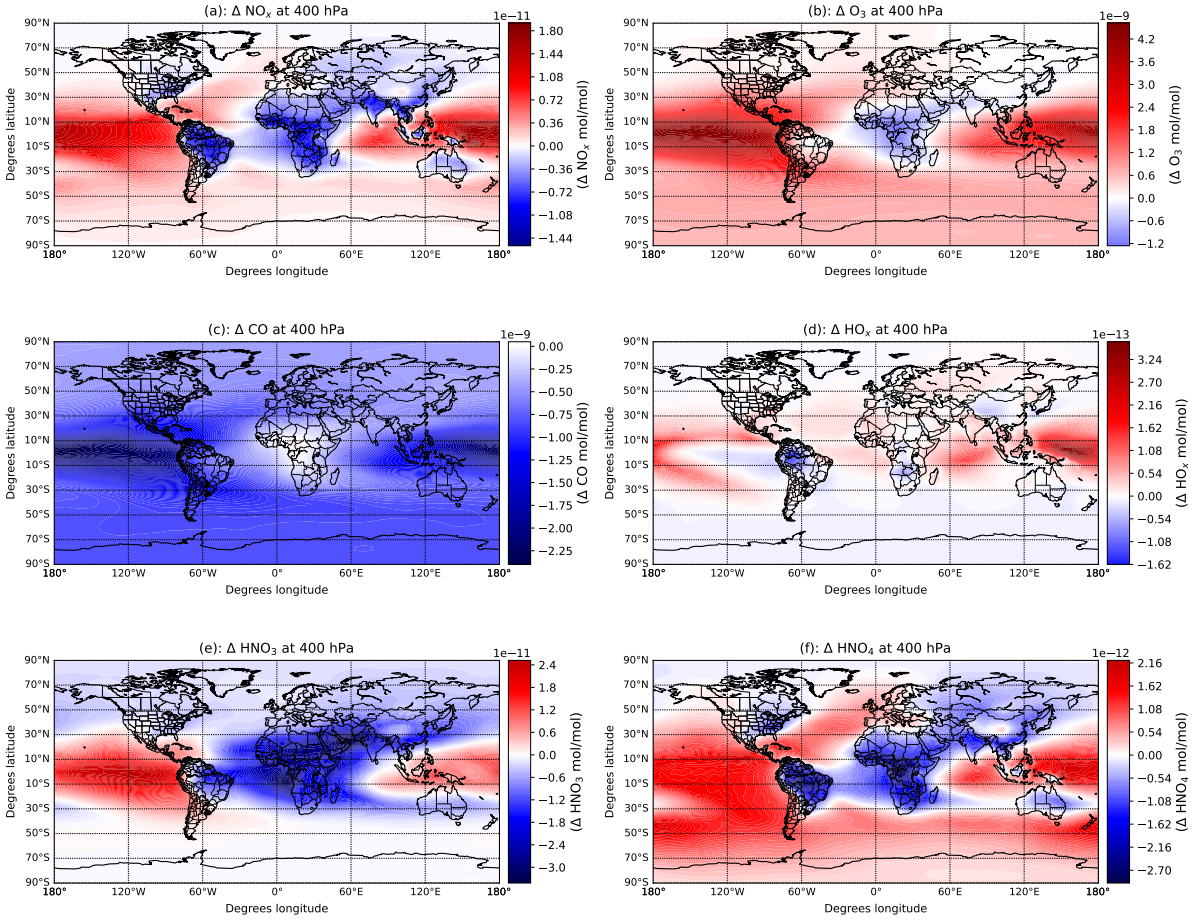

Figure S5. Annually (2002-2007) and globally averaged differences of the NO_x, O_3, CO, HO_x, HNO_3 and HNO_4 mixing ratios between the simulation with the LNO_x based on the flash frequency ($LNOfs_P$) and the simulation with a constant quantity of the LNO_x per flash (CTR_P) at 400 hPa vertical levels.

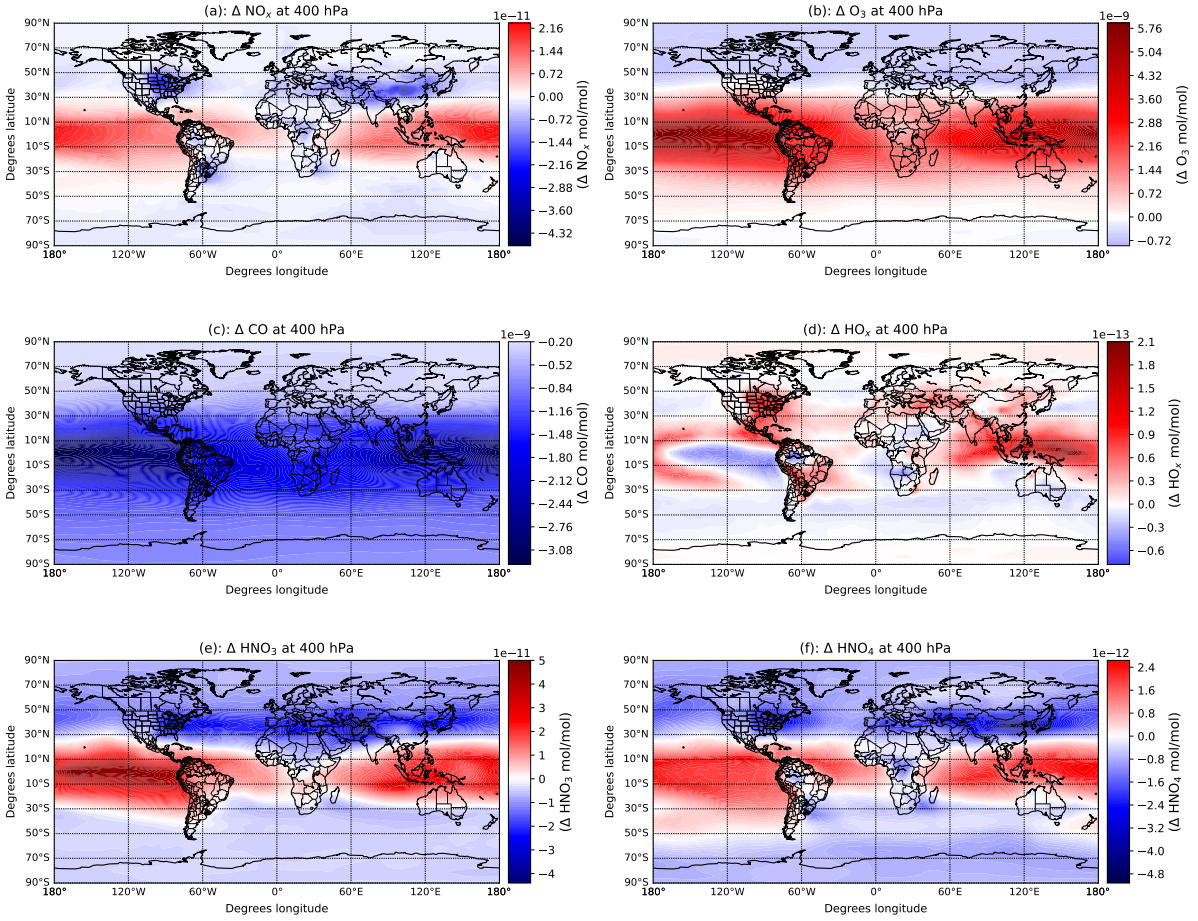

Figure S6. Annually (2002-2007) and globally averaged differences of the NO_x, O_3, CO, HO_x, HNO_3 and HNO_4 mixing ratios between the simulation with the LNO_x based on the flash frequency ($LNOfs_G$) and the simulation with a constant quantity of the LNO_x per flash (CTR_G) at 400 hPa vertical levels.

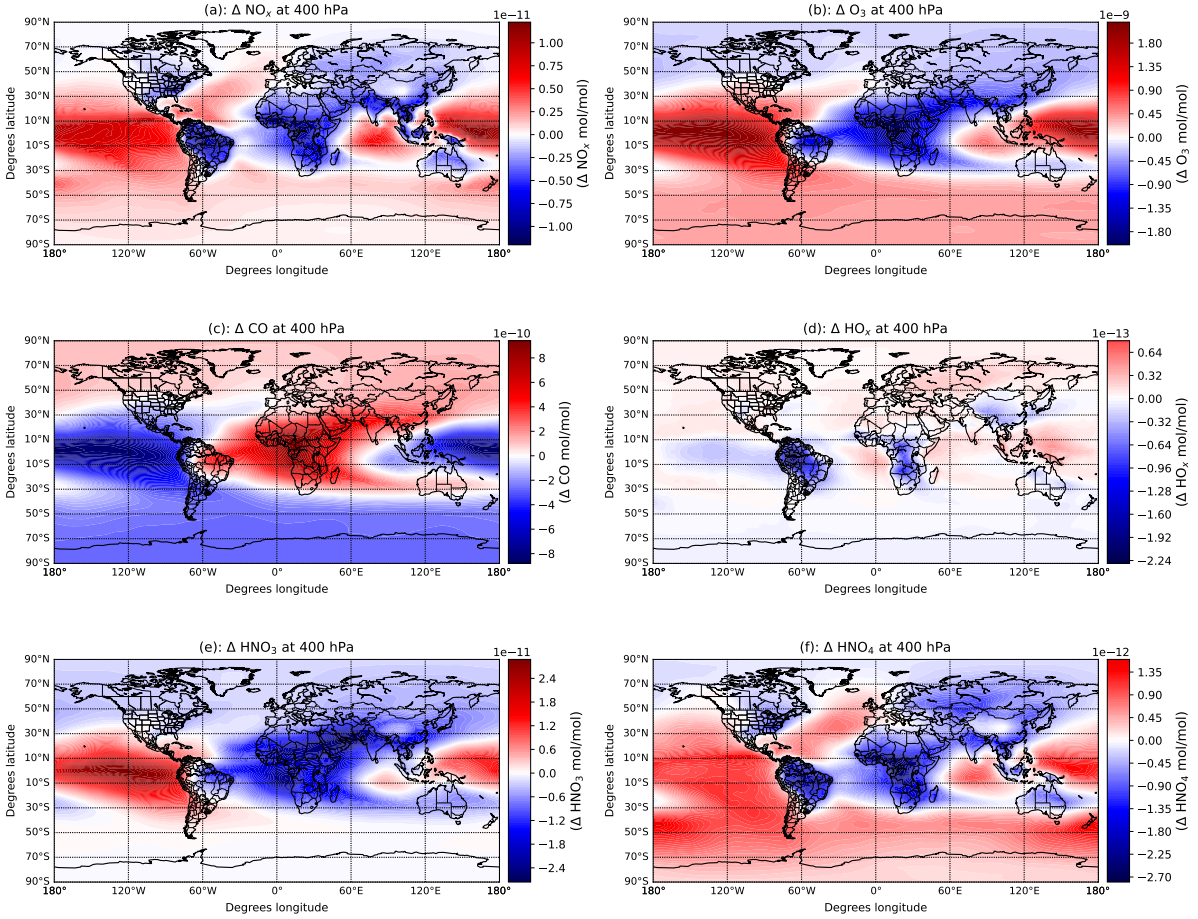

Figure S7. Annually (2002-2007) and globally averaged differences of the NO_x, O_3, CO, HO_x, HNO_3 and HNO_4 mixing ratios between the simulation with the LNO_x based on the flash frequency ($LNOfs_L$) and the simulation with a constant quantity of the LNO_x per flash (CTR_L) at 400 hPa vertical levels.

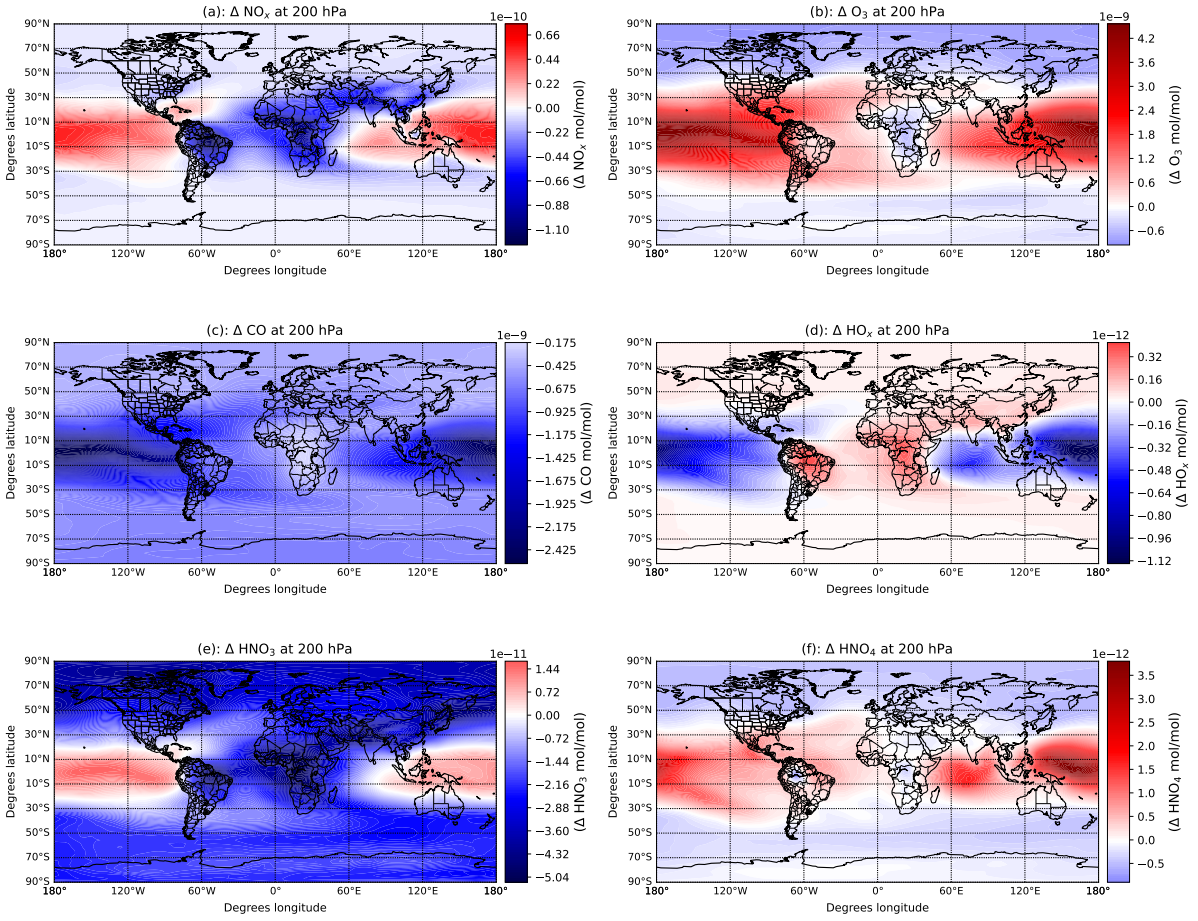

Figure S8. Annually (2002-2007) and globally averaged differences of the NO_x, O_3, CO, HO_x, HNO_3 and HNO_4 mixing ratios between the simulation with the LNO_x based on the flash frequency ($LNOfs_P$) and the simulation with a constant quantity of the LNO_x per flash (CTR_P) at 200 hPa vertical levels.

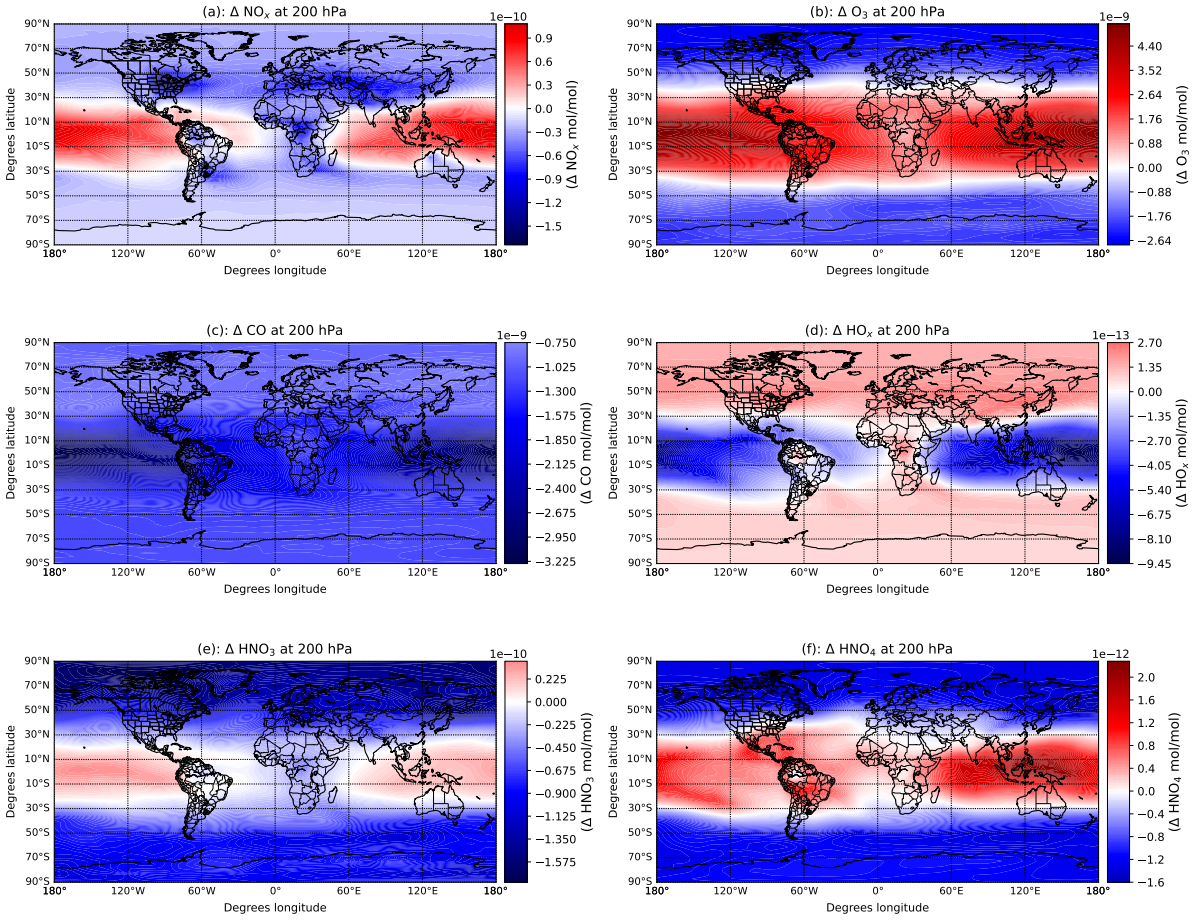

Figure S9. Annually (2002-2007) and globally averaged differences of the NO_x, O_3, CO, HO_x, HNO_3 and HNO_4 mixing ratios between the simulation with the LNO_x based on the flash frequency ($LNOfs_G$) and the simulation with a constant quantity of the LNO_x per flash (CTR_G) at 200 hPa vertical levels.

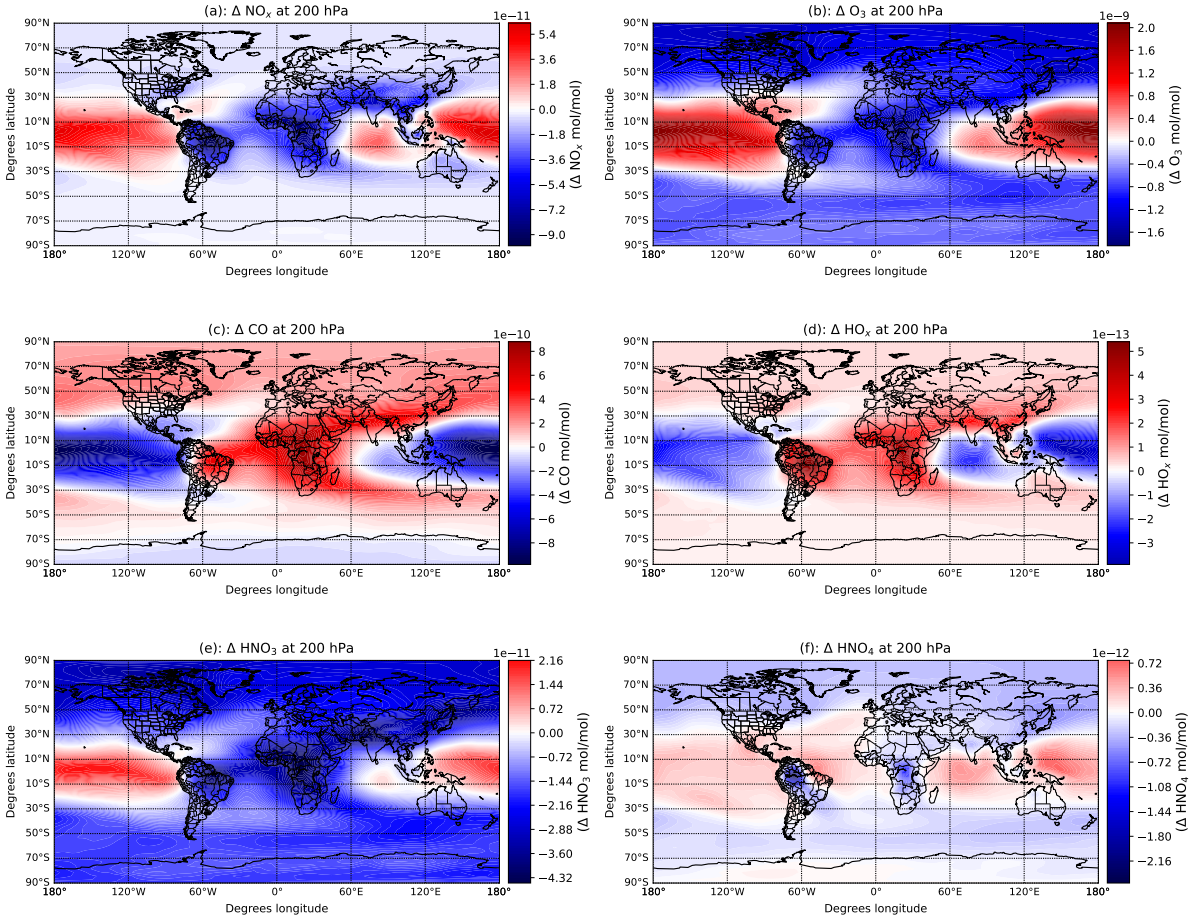

Figure S10. Annually (2002-2007) and globally averaged differences of the NO_x, O_3, CO, HO_x, HNO_3 and HNO_4 mixing ratios between the simulation with the LNO_x based on the flash frequency ($LNOfs_L$) and the simulation with a constant quantity of the LNO_x per flash (CTR_L) at 200 hPa vertical levels.

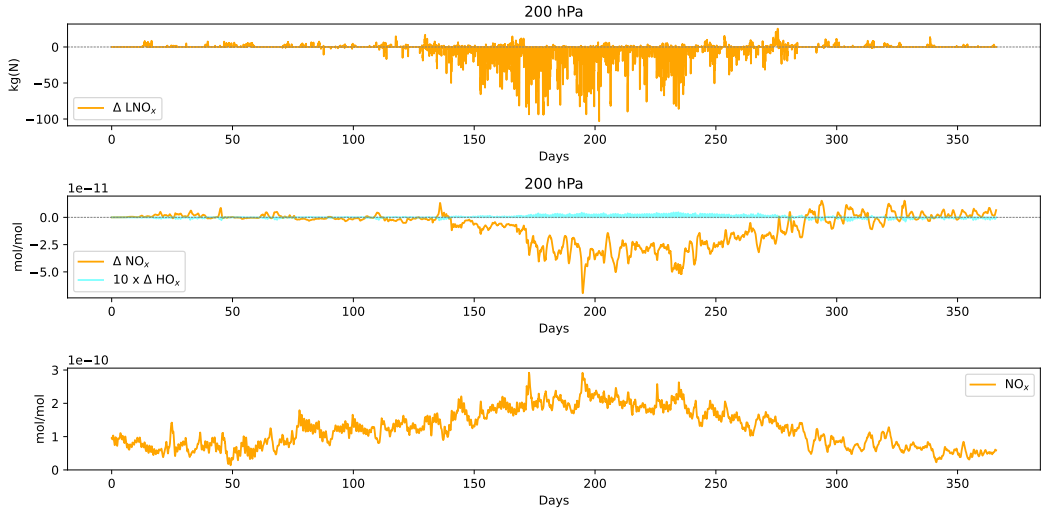

Figure S11. (a): Difference of the hourly total column injection of LNO$_x$ between the LNOfs$_P$ and CTR$_P$ simulations over a 1-year period (day 1 corresponds to 1 January, 2000). (b): Hourly differences of the NO$_x$ and HO$_x$ mixing ratios at 200 hPa. (c): Hourly background mixing ratio of NO$_x$ at the 200 hPa level in the LNOfs$_L$ simulation. The three panels correspond to a spatial average over Europe (bounded by 42°N and 52°N latitude degrees, and 0° to 24°E longitude degrees).

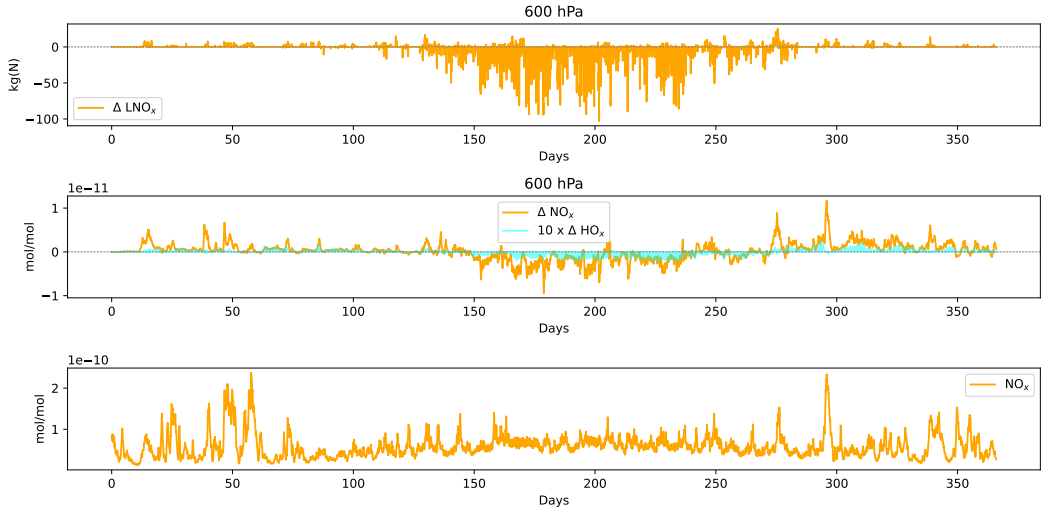

Figure S12. (a): Difference of the hourly total column injection of LNO$_x$ between the LNOfs$_P$ and CTR$_P$ simulations over a 1-year period (day 1 corresponds to 1 January, 2000). (b): Hourly differences of the NO$_x$ and HO$_x$ mixing ratios at 600 hPa. (c): Hourly background mixing ratio of NO$_x$ at the 600 hPa level in the LNOfs$_L$ simulation. The three panels correspond to a spatial average over Europe (bounded by 42°N and 52°N latitude degrees, and 0° to 24°E longitude degrees).

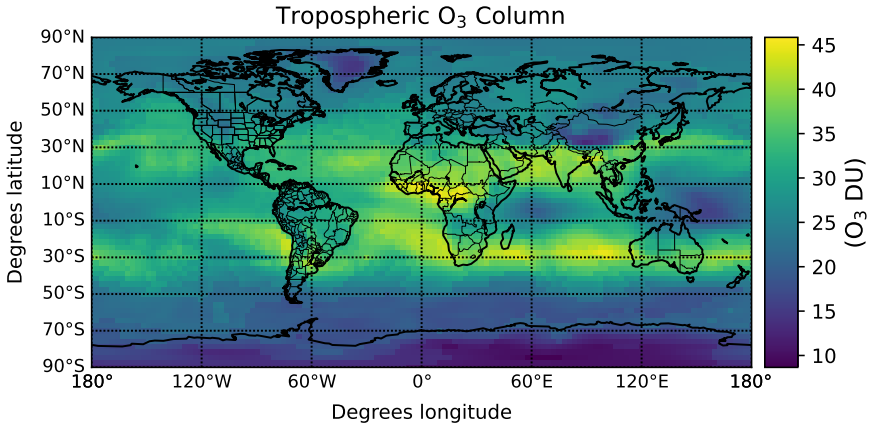

Figure S13. Monthly (January 2004) and globally averaged tropospheric O_3 column in the CTR simulation, including the parameterization of lightning by Grewe et al. (2001) and a constant quantity of the LNO_x per flash (Price et al., 1997).

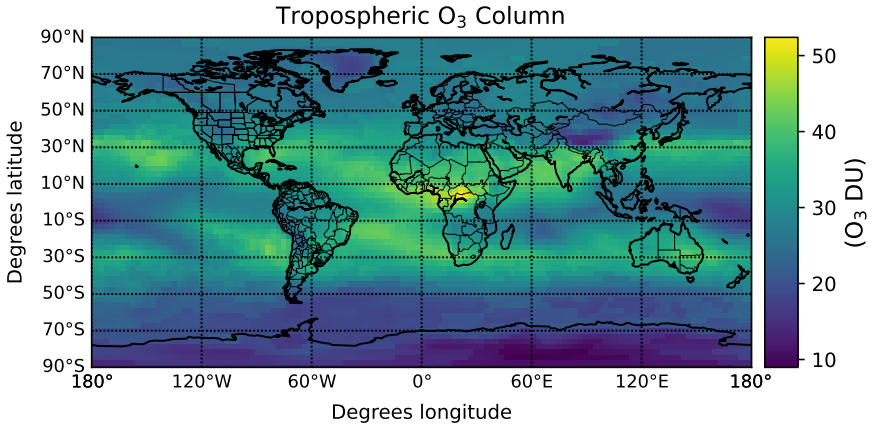

Figure S14. Monthly (February 2004) and globally averaged tropospheric O_3 column in the CTR simulation, including the parameterization of lightning by Grewe et al. (2001) and a constant quantity of the LNO_x per flash (Price et al., 1997).

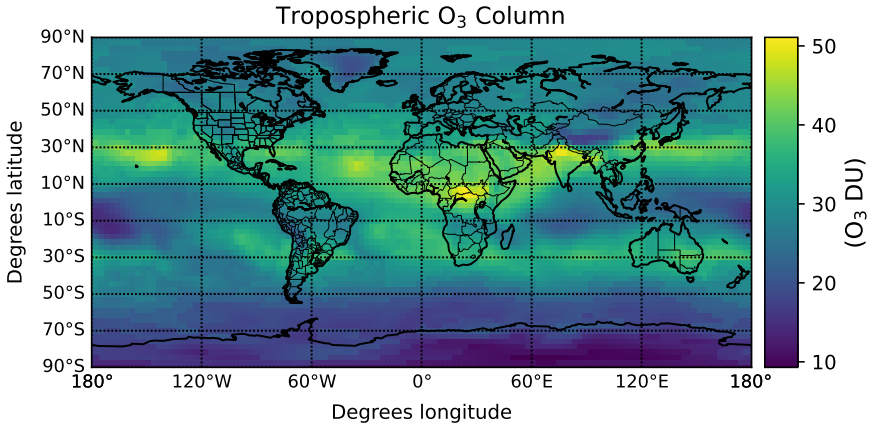

Figure S15. Monthly (March 2004) and globally averaged tropospheric O_3 column in the CTR simulation, including the parameterization of lightning by Grewe et al. (2001) and a constant quantity of the LNO_x per flash (Price et al., 1997).

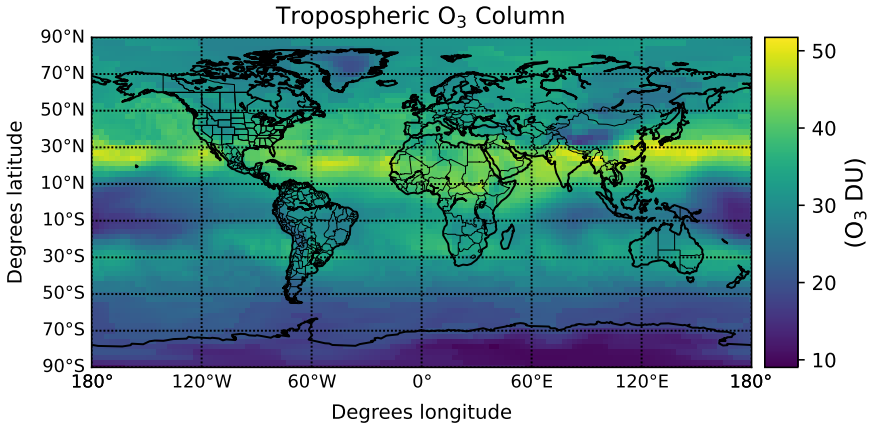

Figure S16. Monthly (April 2004) and globally averaged tropospheric O_3 column in the CTR simulation, including the parameterization of lightning by Grewe et al. (2001) and a constant quantity of the LNO_x per flash (Price et al., 1997).

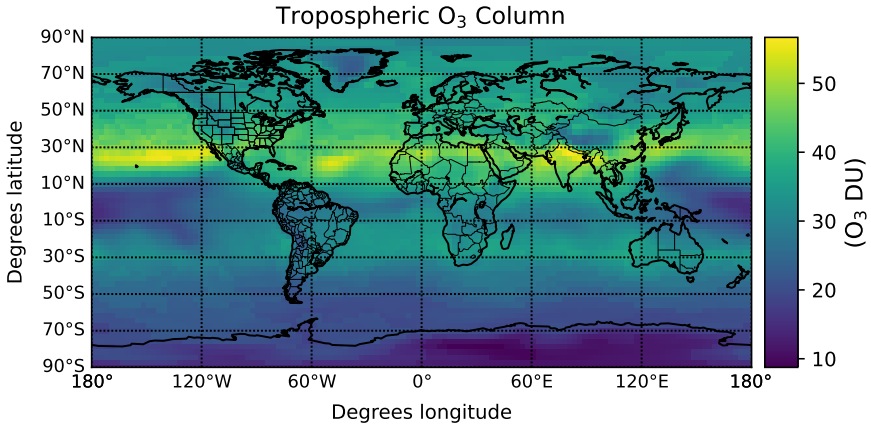

Figure S17. Monthly (May 2004) and globally averaged tropospheric O_3 column in the CTR simulation, including the parameterization of lightning by Grewe et al. (2001) and a constant quantity of the LNO_x per flash (Price et al., 1997).

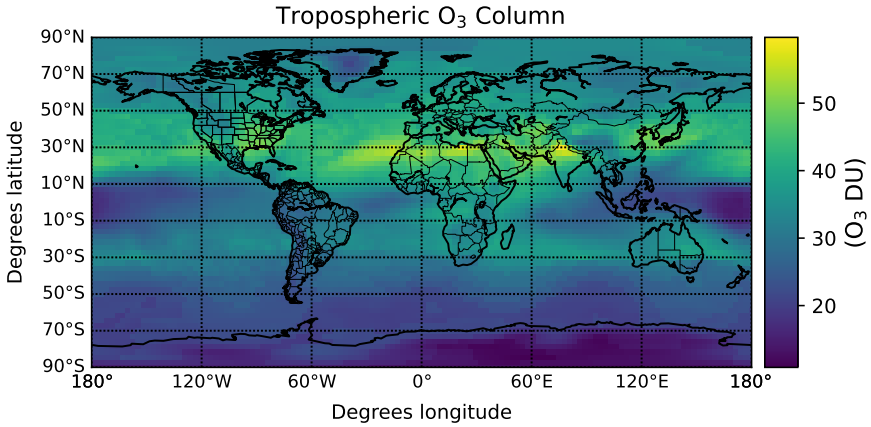

Figure S18. Monthly (June 2004) and globally averaged tropospheric O_3 column in the CTR simulation, including the parameterization of lightning by Grewe et al. (2001) and a constant quantity of the LNO_x per flash (Price et al., 1997).

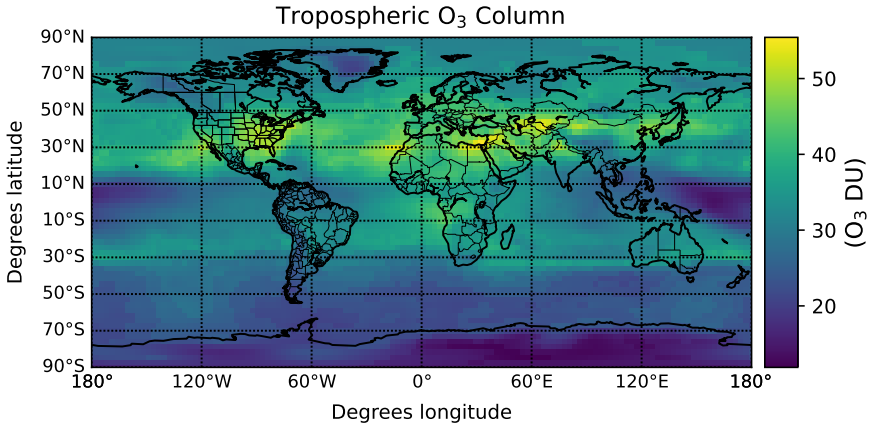

Figure S19. Monthly (July 2004) and globally averaged tropospheric O_3 column in the CTR simulation, including the parameterization of lightning by Grewe et al. (2001) and a constant quantity of the LNO_x per flash (Price et al., 1997).

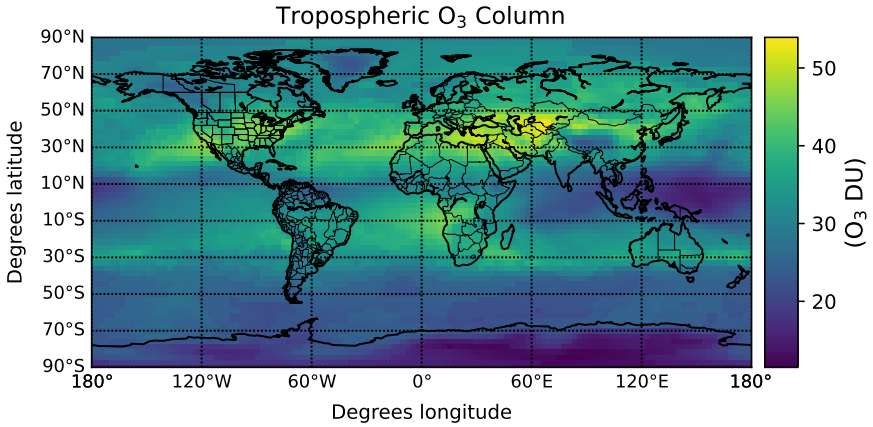

Figure S20. Monthly (August 2004) and globally averaged tropospheric O_3 column in the CTR simulation, including the parameterization of lightning by Grewe et al. (2001) and a constant quantity of the LNO_x per flash (Price et al., 1997).

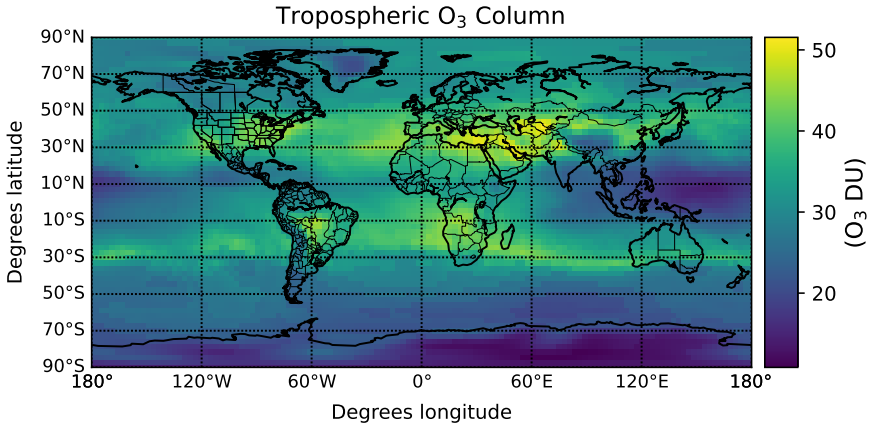

Figure S21. Monthly (September 2004) and globally averaged tropospheric O_3 column in the CTR simulation, including the parameterization of lightning by Grewe et al. (2001) and a constant quantity of the LNO_x per flash (Price et al., 1997).

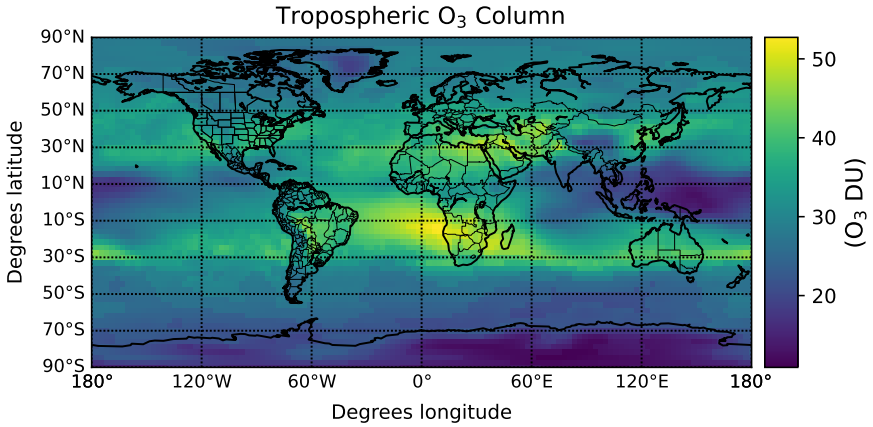

Figure S22. Monthly (October 2004) and globally averaged tropospheric O_3 column in the CTR simulation, including the parameterization of lightning by Grewe et al. (2001) and a constant quantity of the LNO_x per flash (Price et al., 1997).

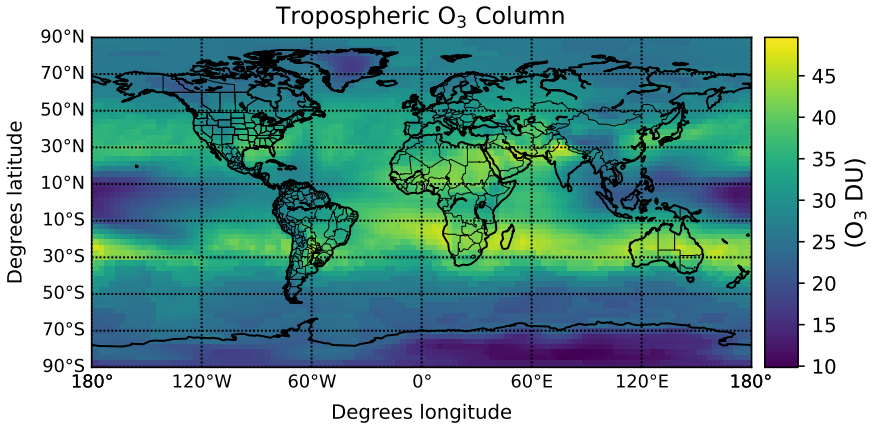

Figure S23. Monthly (November 2004) and globally averaged tropospheric O_3 column in the CTR simulation, including the parameterization of lightning by Grewe et al. (2001) and a constant quantity of the LNO_x per flash (Price et al., 1997).

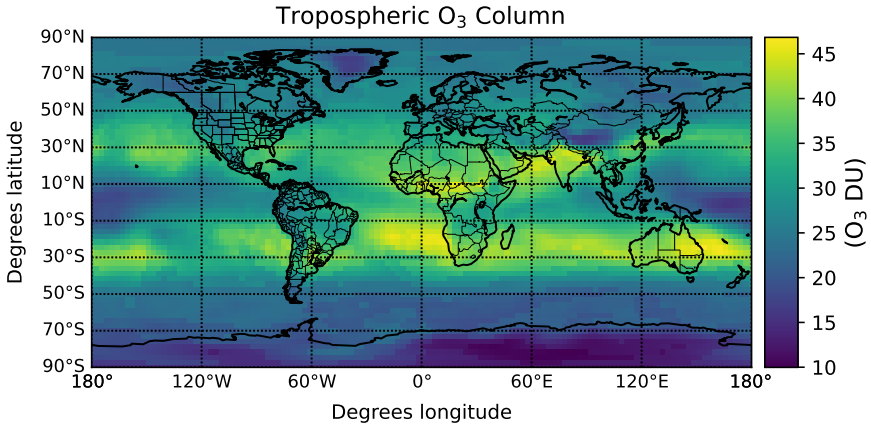

Figure S24. Monthly (December 2004) and globally averaged tropospheric O_3 column in the CTR simulation, including the parameterization of lightning by Grewe et al. (2001) and a constant quantity of the LNO_x per flash (Price et al., 1997).

References

Bucsela, E. J., Pickering, K. E., Allen, D. J., Holzworth, R. H., and Krotkov, N. A.: Midlatitude lightning NO_x production efficiency inferred from OMI and WWLLN data, J. Geophys. Res. Atmos., 124, 13 475–13 497, https://doi.org/10.1029/2018JD029824, 2019.

Grewe, V., Brunner, D., Dameris, M., Grenfell, J., Hein, R., Shindell, D., and Staehelin, J.: Origin and variability of upper tropospheric nitrogen oxides and ozone at northern mid-latitudes, Atmos. Environ., 35, 3421–3433, https://doi.org/10.1016/S1352-2310(01)00134-0, 2001.

Price, C., Penner, J., and Prather, M.: NO_x from lightning: 1. Global distribution based on lightning physics, J. Geophys. Res., 102, 5929, https://doi.org/10.1029/96JD03504, 1997.